Ab initio design of CsSn($X_x Y_{1-x}$)$_3$ (X and Y = Cl, Br, and I) perovskites for photovoltaics

 Arpan Krishna Deb, and Vijay Kumar

COLLECTIONS

Paper published as part of the special topic on Chemical Physics, Energy, Fluids and Plasmas, Materials Science and Mathematical Physics

View Online   Export Citation   CrossMark

ARTICLES YOU MAY BE INTERESTED IN

Synthesis and characterization of $CsSnI_3$ thin films
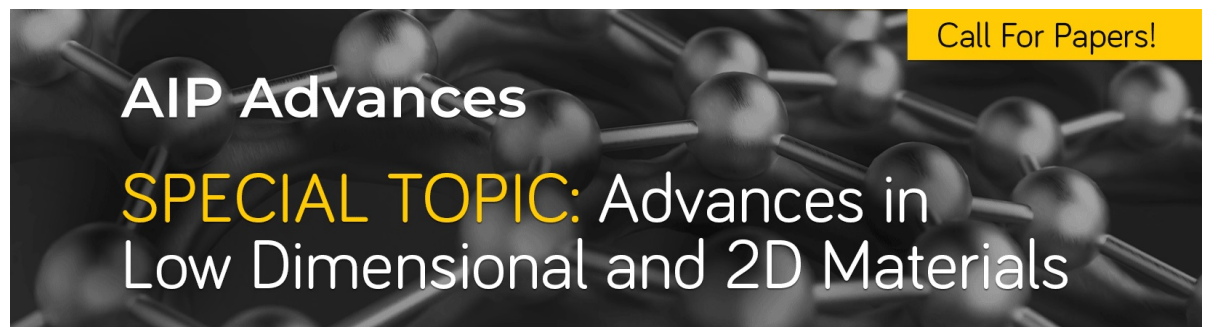Applied Physics Letters **96**, 221903 (2010); https://doi.org/10.1063/1.3442511

Detailed Balance Limit of Efficiency of p-n Junction Solar Cells
Journal of Applied Physics **32**, 510 (1961); https://doi.org/10.1063/1.1736034

Unusual defect physics in $CH_3NH_3PbI_3$ perovskite solar cell absorber
Applied Physics Letters **104**, 063903 (2014); https://doi.org/10.1063/1.4864778

Call For Papers!

AIP Advances

SPECIAL TOPIC: Advances in Low Dimensional and 2D Materials

Ab initio design of CsSn(X$_x$Y$_{1−x}$)$_3$ (X and Y = Cl, Br, and I) perovskites for photovoltaics

Arpan Krishna Deb[1] and Vijay Kumar[1,2]

[1]*Center for Informatics, School of Natural Sciences, Shiv Nadar University, NH91, Tehsil Dadri, Gautam Buddha Nagar -201314, Uttar Pradesh, India*
[2]*Dr. Vijay Kumar Foundation, 1969 Sector 4, Gurgaon 122001, Haryana, India*

Ab initio calculations on CsSnX$_3$ perovskites and mixed halides CsSn(X$_x$Y$_{1-x}$)$_3$, X and Y = I, Cl, and Br, show that all of them have a *direct* band gap of ~1 eV which can be tuned by varying the compositions of X and Y. The optimized supercells are tetragonal, orthorhombic or monoclinic. The top of the valence band arises from hybridization of Sn 4s and halogen p valence orbitals while the bottom of the conduction band has predominantly Sn *p* character. Similar to organo-metallic lead halides this is expected to facilitate *p-p* optical transitions that are highly favourable for photoabsorption. Our results suggest that these inorganic perovskites have the desired features to achieve high efficiency of photo-response with appropriate combination of halogens. © 2015 Author(s). All article content, except where otherwise noted, is licensed under a Creative Commons Attribution 3.0 Unported License. [http://dx.doi.org/10.1063/1.4927503]

Great efforts are being made to develop materials that can convert abundant solar energy in to electrical energy efficiently and economically to save environment from burning of fossil fuels. Moreover, reserves of fossil fuels are getting depleted and therefore alternate energy sources are required. Recently high efficiency of ~15-20% has been achieved with CH$_3$NH$_3$PbI$_3$ perovskite as light absorber.[1–9] This has created great excitement and raised hopes of making solar energy cheap due to the self-assembling character[10] and ease of making the nanocrystals. An understanding of the electronic properties of these perovskites is fundamental to achieve greatly improved performance of photovoltaic devices. The organo-metallic halides lack stability and improved materials are desireable.[11] Here we report results on inorganic halides, CsSn(X-Y)$_3$, (X and Y = halides) and show that they also have the potential to achieve high efficiency of photo-conversion.

There are several factors that make CH$_3$NH$_3$PbI$_3$ type perovskites so interesting.[12–14] 1) There is a direct band gap of about 1-1.5 eV and this is very good for high optical absorption of solar radiation. 2) It is reported that there are *p-p* optical transitions that are favourable because the Pb atoms behave as divalent and their 5s states do not lose their s electrons though they hybridize significantly with the halogen p states. Hence the lower parts of the CBs of organo-lead halides are mainly made up of the unoccupied Pb 5p orbitals while the top of the VB mainly comprises the halogen p orbitals mixed with significant component of Pb 5s orbital. 3) These halides exhibit ambipolar charge transport and very long electron hole diffusion lengths. The effective masses of the electrons and holes are small and also the electron-hole binding energy is small. Further improvements have been obtained by manipulating the chemical composition by substitution of e.g. Cl in place of iodine to form a mixed organo-metallic halide that has been found to improve the efficiency and the stability of the solar cells.[4,6,8,15] Other combinations of halogens in these mixed organo-metallic halides have also been found promising. Experiments[16] show that the band gap of (CH$_3$NH$_3$)Pb(Br$_{1-x}$Cl$_x$)$_3$ single crystals increases and the unit cell dimensions decrease with an increase in Cl content *x*. Our results on inorganic perovskites support this finding.

Among the inorganic perovskites, CsSnI$_3$ is promising as it is lead free and has the potential to have all the above mentioned properties of organo-metallic perovskites. Experiments have shown near-infrared emission at room temperature.[17] This makes it an important candidate for photovoltaic

applications. The experimental optical band gap is reported to be 1.3 eV[17] and the theoretical value lies in the range[18] of 0.35 to 0.56 eV depending on the phase. Another experimental study has reported strikingly high photoresponse in a derivative of $CsSnI_3$ viz. $CsSnI_2Cl$ but $CsSnBr_2I$ shows practically no photoresponse.[19,20] This is a strong motivation to investigate the electronic structure of some derivatives of $CsSnI_3$ and other mixed halides to understand and predict newer photovoltaic materials. Here we report results of the atomic and electronic structure of $CsSn(X_xY_{1-x})_3$ perovskites with X and Y = I, Cl, and Br. The band gap of these materials is calculated to be direct and can be tuned around the value of ~0.75-1.3 eV that makes them attractive for photovoltaic applications. Among the several distributions of mixed halides we studied, we find some competing configurations with significant changes in the atomic structure, cell dimensions, and band gap depending upon the distribution of X and Y. These results suggest that there could be different behaviours of the same material depending upon the distribution of anionic substitution and how samples are made.

We performed *ab initio* calculations using projector-augmented wave (PAW)[21,22] pseudopotential method and generalized gradient approximation (GGA)[23] for the exchange-correlation energy as implemented in Vienna Ab initio Simulation Program (VASP). The pseudopotential for Sn is chosen to include *d* electrons as part of the valence. A 2x2x2 cubic supercell of $CsSnI_3$ with 40 atoms has been considered to study the atomic and electronic structure of mixed halides $CsSnI_2Cl$, $CsSnBr_2I$, $CsSnI_2Br$, and $CsSnBr_2Cl$, and the effects of different distributions of Br, Cl, and I atoms in the supercell. The Brillouin zone is sampled with 5x5x5 Monkhorst–Pack[24] **k**-points. The lattice parameters as well as the atomic positions within the supercell have been optimized till the forces and total energy are converged within 0.005 eV/Å and 10^{-5} eV, respectively. We considered several configurations of halogen atoms in $CsSn(X-Y)_3$ within the cubic supercell. Firstly we can divide the halogen sites (centers of faces) in the unit cell in to three sublattices each having two atoms on the opposite faces in the unit cell and occupy one of the sublattices with one type of halogen to obtain an 'ordered' distribution of X and Y. 'Ordered' structures can also be created starting from a supercell such as 1x1x2 or 1x2x2 in which one can have ordered structure in the *x* and *y* or the *x* direction. Another way is to distribute the halogen atoms X and Y randomly in the 40 atom supercell creating a 'disordered' distribution. Here we present results of some low lying optimized configurations of the ordered and disordered mixed perovskites.

First we optimized the atomic structure of cubic $CsSnI_3$, $CsSnBr_3$, and $CsSnCl_3$ perovskites. For this we also used a 2x2x2 supercell as for the mixed halides in order to keep the computational accuracy nearly the same for all calculations. The optimized supercells as well as the energy bands are shown in Fig. 1. There is a *direct* band gap of 0.45 eV, 0.62 eV, and 1.01 eV at the Γ point and the cohesive energy is 2.625, 2.795, and 3.097 eV/atom while the Sn-X bond length is 3.13 Å, 2.95 Å, and 2.81 Å for X = I, Br, and Cl, respectively. The band structure plots reported here are calculated from a 40-atom supercell. Earlier calculations on $CsSnI_3$, $CsSnBr_3$, and $CsSnCl_3$ perovskites show a direct band gap at the R point. It is noteworthy here that for a 2x2x2 supercell the Γ point coincides with the R point of the unit cell and therefore the band gap in our plots appears at the Γ point. The lattice parameter for the cubic phase of $CsSnX_3$ (X = I, Br, and Cl,) is 6.259 Å, 5.872 Å, 5.614 Å, in good agreement with the theoretical values[18,25] of 6.219 Å, 5.804 Å, 5.56 Å, respectively obtained earlier. The band gap and cohesive energy increase in going from $CsSnI_3$ to $CsSnCl_3$. This is due to the fact that the bonding in these systems is dominated by Coulomb interactions and since Br and Cl are smaller in size than I, the shorter Sn-Br and Sn-Cl bonds lead to stronger bonding in the former. Also the 2*p* and 3*p* electronic levels of Cl and Br lie deeper in energy than the 4*p* level of I. This gives rise to an increase in the band gap. The top of the VB has mixed *s-p* character and the bottom of the CB has *p* character of Sn similar to the organic perovskites and this makes the *p-p* optical transitions very likely in these inorganic perovskites also. The band gap is underestimated in GGA and the obtained values suggest that these perovskites are interesting for solar energy applications.

For the mixed perovskites we studied several distributions of X and Y in each case of $CsSnI_2Cl$, $CsSnI_2Br$, $CsSnBr_2Cl$, and $CsSnBr_2I$ and the results of the optimized structures are given in Tables SI-SIV in supplementary material.[26] In Table I we have given the results of the cohesive energy, band gap, Sn-X bond lengths and lattice parameters for the two lowest lying configurations
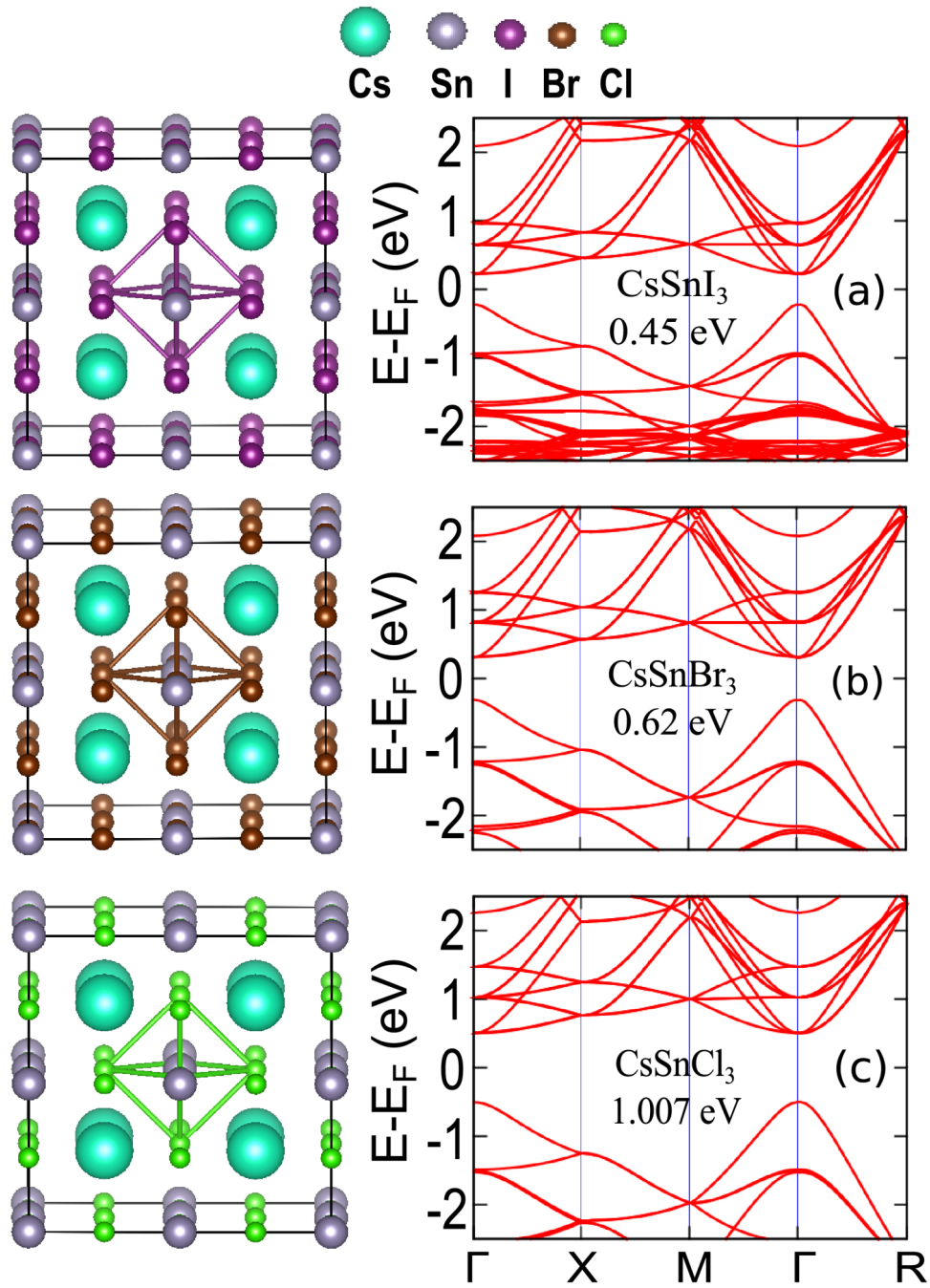
FIG. 1. A 2x2x2 supercell of the optimized atomic structure of $CsSnX_3$ inorganic halide with X = (a) I, (b) Br, and (c) Cl and the respective electronic band structure. The value of the direct band gap at the Γ point is given.

(1 and 2). For $CsSnI_2Cl$ and $CsSnI_2Br$, the configuration derived from a disordered distribution of X and Y has the lowest energy while the one derived from an ordered distribution of X and Y is the second best. But for $CsSnBr_2Cl$ and $CsSnBr_2I$, the lowest energy configuration is an ordered structure. It seems that a large difference in the ionic radii of the halogens favors disordered structures. Interestingly we find that in all the cases there is a direct band gap at the Γ point. As Table I shows, the value of the band gap varies as X and Y are changed and is underestimated within GGA. The optimized structures of the lowest lying configurations have orthorhombic structure with a tendency

TABLE I. Cohesive energy (E_c in eV/atom), band gap (E_g), Sn-X and Sn-Y bond lengths (d_{Sn-X} and d_{Sn-Y}), and lattice parameters of the two lowest lying configurations (1 corresponds to the lowest while 2, the 2nd lowest in energy) of $CsSn(X-Y)_3$ perovskites. For X = I and Y = Cl and Br, respectively in $CsSnI_2Cl$ and $CsSnI_2Br$, and for X = Br and Y = I and Cl, respectively in $CsSnBr_2Cl$ and $CsSnBr_2I$.

Systems		E_c	E_g (eV)	d_{Sn-X} (Å)	d_{Sn-Y} (Å)	Lattice parameters					
						a (Å)	b (Å)	c (Å)	α (°)	β (°)	γ (°)
$CsSnI_2Cl$	1	2.777	0.92	2.99-3.61	2.52-2.53	12.76	11.54	12.28	90	90	90
	2	2.771	0.99	2.98-3.60	2.52-2.55	12.64	11.97	12.24	90	92	90
$CsSnI_2Br$	1	2.677	0.78	3.07-3.54	2.76	12.76	11.85	12.26	90	90	90
	2	2.658	0.45	3.15	2.79-2.81	12.15	12.15	11.57	90	90	90
$CsSnBr_2I$	1	2.737	0.99	2.69	2.79-3.36	12.28	12.01	11.93	90	90	90
	2	2.726	0.55	2.78	2.96	12.18	12.18	12.74	90	90	90
$CsSnBr_2Cl$	1	2.895	1.08	2.8-3.31	2.64-2.65	11.94	11.50	11.58	91	90	90
	2	2.854	1.27	2.79-3.29	2.62	11.38	11.58	12.04	90	90	90

to become monoclinic in some cases and are shown in Fig. 2 while their energy bands and the density of states are shown in Fig. 3.

Table I shows that the cohesive energy varies from 2.677 to 2.895 eV/atom and the direct band gap at the Γ point (Fig. 3) varies from 0.78 eV to 1.08 eV in the lowest energy configurations of
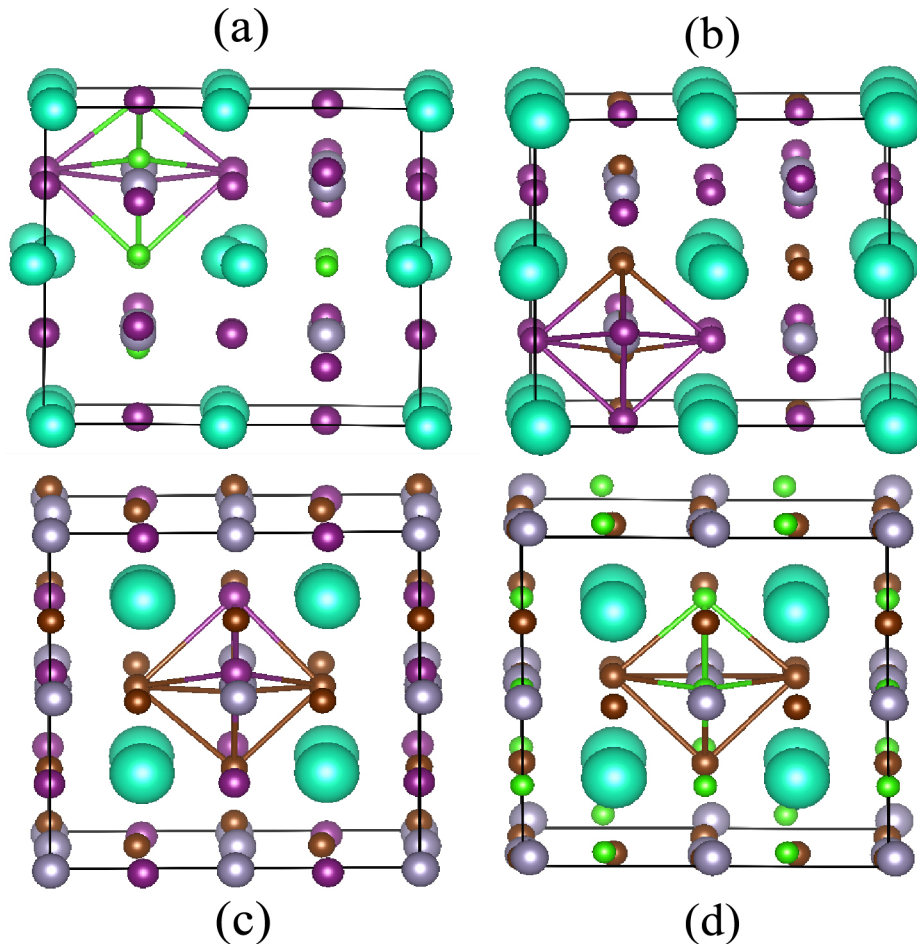

FIG. 2. A 40-atom supercell of the lowest energy configuration of (a) $CsSnI_2Cl$ (orthorhombic), (b) $CsSnI_2Br$ (orthorhombic), (c) $CsSnBr_2I$ (orthorhombic), and (d) $CsSnBr_2Cl$ (monoclinic).
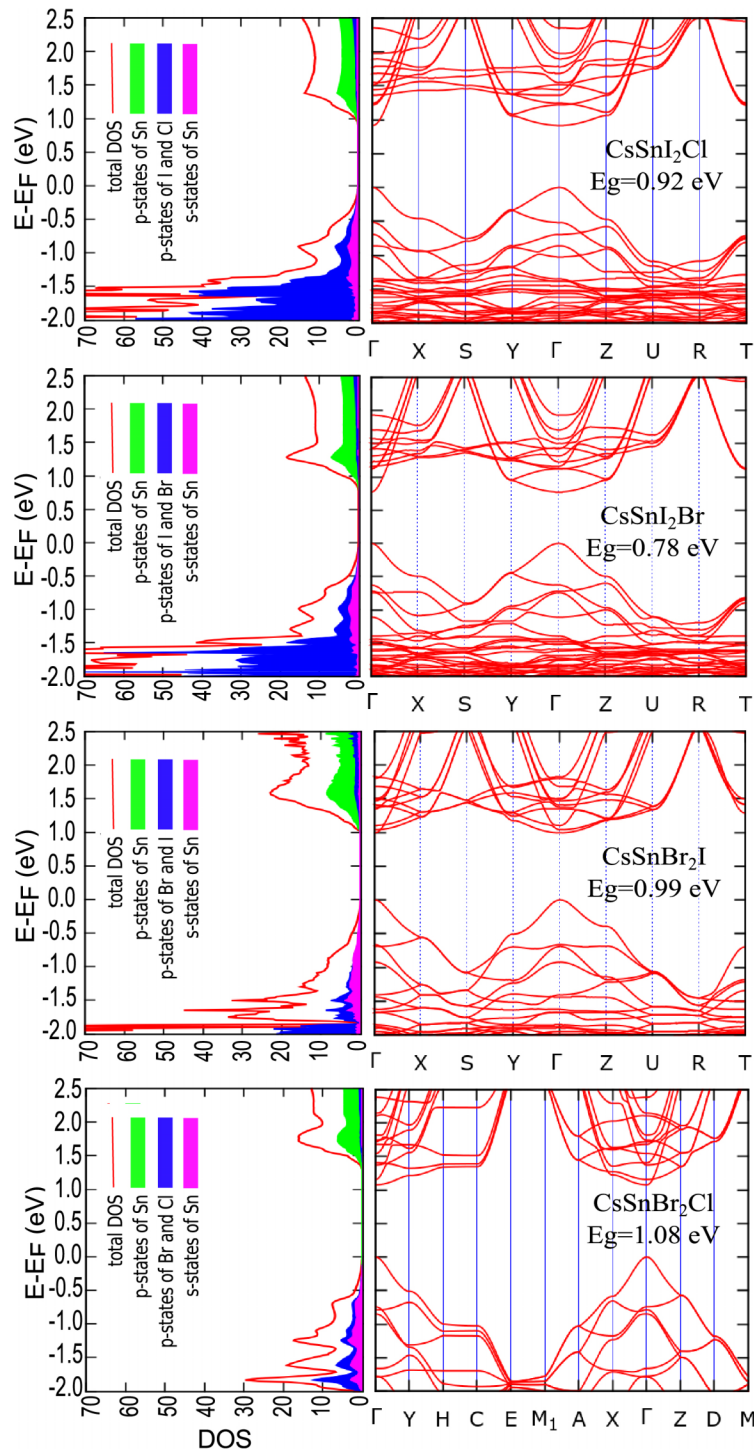
FIG. 3. Electronic band structure and density of states (DOS) for the lowest energy configurations of CsSnI$_2$Cl, CsSnI$_2$Br, CsSnBr$_2$I, and CsSnBr$_2$Cl. The band gap, E$_g$, is direct at the Γ point in all cases. The partial DOS arising from the *s and p* states of Sn and *p* states of halogens are also shown.

the different systems. The band gap can be tuned by suitably varying the composition and halogens. As the band gap in GGA is underestimated, the true values are likely to fall in the range of about 1 – 1.5 eV which is desirable. The largest cohesive energy of 2.895 eV/atom is obtained for CsSnBr$_2$Cl. We calculated the formation energies of the lowest energy configurations of all

the mixed halides with the formula, $\Delta H = E(CsSn(X_xY_{1-x})_3) - \{xE(CsSnX_3) + (1-x)E(CsSnY_3)\}$. Here $E(CsSn(X_xY_{1-x})_3)$, $E(CsSnX_3)$ and $E(CsSnY_3)$ are the total energies of the mixed halide and the pure halides, respectively. For the lowest energy configurations of $CsSnI_2Cl$, $CsSnI_2Br$, $CsSnBr_2Cl$, and $CsSnBr_2I$, the formation energies are very close to 0.0 eV. Hence these mixed halides should form. In general the lattice parameters tend to reduce when a smaller anion is added as it is also observed for $CH_3NH_3Pb(Br_{1-x}Cl_x)_3$. The d_{Sn-Cl} value is the shortest in $CsSnI_2Cl$ and in general has small variation. A similar behaviour is obtained for X = Br and Y = I in which case d_{Sn-Br} shows a small variation and it is shorter compared with d_{Sn-I}, but in the case of $CsSnBr_2Cl$, d_{Sn-Br} shows a large variation. Further, d_{Sn-Br} also has small variation in $CsSnBr_2I$. This suggests that in mixed halides, in general the smaller halogen atom has small variation in the bond length with Sn, while the bond with larger halogen has large variation. This can be understood from the fact that the shorter bonds are also the stronger ones and the system accommodates strain due to size mismatch by varying the lengths of the weaker bonds. It is also noted that the d_{Sn-Cl} values in $CsSnI_2Cl$ and $CsSnBr_2Cl$ are shorter than 2.81 Å in the pure $CsSnCl_3$. A similar behaviour is obtained for d_{Sn-Br} bonds for $CsSnI_2$ Br case. The smaller value of the d_{Sn-Cl} and d_{Sn-Br} bonds suggests some covalent character of bonding. We performed Bader charge analysis for the pure and mixed halide systems according to which the valence charge on Sn atom lies in the range of 12.8 -13.3 electrons compared with 14 e taken in a free atom. This means that the bonding is not fully ionic and there is some covalent bonding character between Sn and X (Y). The higher values of charge correspond to the cases where the distortion is more whereas the lower values are from the less distorted cases. As it can be seen in Fig. 3, the top of the VB in these mixed halides is formed of *p* electrons of the halogens that hybridize with the *5s* electrons of Sn while the bottom of the CB is formed of the *p* orbitals of Sn *which behaves like a divalent atom in these compounds*. Therefore these materials are also expected to have the desired and favorable *p-p* optical transitions similar to the organo-metallic halides.

The nearly zero heat of formation suggests the possibility of random distribution of halogens in mixed halides. Configuration 1 of $CsSnI_2Cl$ arises from a disordered configuration, but Table I shows that the second lowest energy configuration of $CsSnI_2Cl$ arising from an ordered configuration is almost degenerate with configuration 1 and both have comparable GGA band gaps as well as d_{Sn-Cl} and d_{Sn-I} values. However, the supercell dimensions differ significantly. As discussed earlier, the d_{Sn-Cl} values (2.52-2.55 Å) are shorter than 2.81 Å in pure $CsSnCl_3$. Therefore Sn-Cl bonding is stronger in these mixed halides. Also d_{Sn-I} has large variation (2.98-3.61 Å) compared to 3.13 Å in $CsSnI_3$ but the shorter bonds are more in number. The shorter Sn-Cl bonds and large variation in Sn-I bond lengths give stability to the structure with significantly different sizes of Cl and I ions. The average Bader charge on Sn ions is ~13.06 e which suggests covalent nature of bonding in the two low energy configurations of $CsSnI_2Cl$.

The second best configuration of $CsSnI_2Br$ has tetragonal structure and it lies only 19 meV/atom higher in energy than configuration 1. The d_{Sn-I} value is close to that in $CsSnI_3$ while d_{Sn-Br} is only slightly smaller than the value in $CsSnBr_3$. The GGA value of the band gap is smaller (0.45 eV) but the actual value could be close to 1 eV. Also the second best configuration of $CsSnBr_2I$ has tetragonal structure with slightly smaller values of d_{Sn-Br} and d_{Sn-I} than the values in the respective pure halides. This configuration lies only 11 meV/atom higher in energy than configuration 1 with a smaller band gap (0.55 eV). This result suggests a possibility of quite different properties of $CsSnBr_2I$ depending upon how this compound is prepared, but for $CsSnI_2Cl$, the variation in properties is smaller. For $CsSnBr_2Cl$ the GGA band gap of the two low lying configurations is large (1.08 eV and 1.27 eV). In both the configurations, there is a lot of distortion and d_{Sn-Cl} is shorter than in $CsSnCl_3$. In all the cases where there is large distortion, we find more Bader charge on Sn. This suggests partially covalent bonding in these systems and it is also a reason for larger band gaps. Indeed, we find larger band gap in some mixed halides such as $CsSnI_2Br$ than the values in pure cases. For $CsSnI_2Br$ and $CsSnBr_2I$, the lowest energy configurations have GGA band gap of 0.78 and 0.99 eV, respectively, compared with the calculated values of 0.45 eV and 0.62 eV for $CsSnI_3$ and $CsSnBr_3$ cases. The distortion in the bond lengths makes the octahedra of the anions (Fig. S1 - S4 in supplemental material[26]) twisted or rotated. The trend of the distortion due to the bond length optimization and consequent increase in the band gap for all the compounds is shown in the supplementary material

(Tables SI-SIV and Figs. S1-S4).[26] Notably in the 3rd configuration of CsSnI$_2$Br shown in Fig. S2 we can hardly see any distortion of the octahedral cage. The band gap of this configuration is as low as 0.27 eV. Also Table I shows that the cohesive energy is the largest for CsSnBr$_2$Cl closely followed by CsSnI$_2$Cl. This shows that structurally these compounds are more stable than the other ones.

In summary our results suggest that inorganic mixed halides and in particular CsSnI$_2$Cl and CsSnBr$_2$Cl compounds are very promising for photovoltaic applications. In all cases the band gap is direct and it lies in the range of 0.78 - 1.08 eV in the lowest energy configurations suggesting that the actual band gaps might well be in the range of 1- 1.5 eV which is good for solar radiation absorption. The top of the VB and the bottom of the CB have s-p and p character, respectively, similar to the organic lead halide materials and we expect p-p transition in these materials also. The curvature near the band edges signifies low effective masses of the charge carriers. This is also important with respect to the transport of charge and further reduction in the complexity of the making of devices. Therefore these mixed inorganic halides have properties that make them potentially good candidates for photovoltaic applications. The band gap varies depending upon the distribution of the halogens and the optimization of the tin-halogen bond lengths. It is likely that a composite of such materials can have increased photo-absorption. Our results also suggest significant variation in the properties even for closely lying configurations and this could be a reason for the unfavourable results of photo-absorption in the case of CsSnBr$_2$I. We also hope that our results will have bearing on the understanding of the mixed organic lead halides.

[1] N.G. Park, J. Phys. Chem. Lett. **4**, 2423 (2013).
[2] J. Bisquert, J. Phys. Chem. Lett. **4**, 2597 (2013).
[3] A. Kojima, K. Teshima, Y. Shirai, and T. Miyasaka, J. Am. Chem. Soc. **131**, 6050 (2009).
[4] M. M. Lee, J. Teuscher, T. Miyasaka, T. N. Murakami, and H. J. Snaith, Science **338**, 643 (2012).
[5] J. Burschka, N. Pellet, S.J. Moon, R. Humphry-Baker, P. Gao, Md. K. Nazeeruddin, and M. Grätzel, Nature **499**, 316 (2013).
[6] L. Etgar, P. Gao, Z. X. Peng, A. K. Chandiran, B. Liu, Md. K. Nazeeruddin, and M. Grätzel, J. Am. Chem. Soc. **134**, 17396 (2012).
[7] I. Chung, B. Lee, J. He, R. P. H. Chang, and M. G. Kanatzidis, Nature **485**, 486 (2012).
[8] M. Liu, M. B. Johnston, and H. J. Snaith, Nature **501**, 395 (2013).
[9] P.V. Kamat, J. Phys. Chem. Lett. **4**, 3733 (2013).
[10] H. J. Snaith, J. Phys. Chem. Lett. **4**, 3623 (2013).
[11] G. Niu, W. Li, F. Meng, L. Wang, H. Dong, and Y. Qiu, J. Mater. Chem. A **2**, 705 (2014).
[12] W.J. Yin, T. Shi, and Y. Yan, Adv. Mater. **26**, 4653 (2014).
[13] W.J. Yin, T. Shi, and Y. Yan, Appl. Phys. Lett. **104**, 063903 (2014).
[14] J. M. Frost, K. T. Butler, F. Brivio, C. H. Hendon, M. van Schilfgaarde, and A. Walsh, Nano Lett. **14**, 2584 (2014).
[15] S. Colella, E. Mosconi, P. Fedeli, A. Listorti, F. Gazza, F. Orlandi, P. Ferro, T. Besagni, A. Rizzo, F. Calestani, G. Gigli, F. De Angelis, and R. Mosca, Chem. Mater. **25**, 4613 (2013).
[16] T. Zhang, M. Yang, E. E. Benson, Z. Li, J. van de Lagemaat, J. M. Luther, Y. Yan, K. Zhu, and Y. Zhao, Chem. Commun. **51**, 7820 (2015).
[17] I. Chung, B. Lee, J. He, R.P. H. Chang, and M.G. Kanatzidis, Nature **485**, 486 (2012).
[18] I. Borriello, G. Cantele, and D. Ninno, Phys. Rev. B **77**, 235214 (2008).
[19] M.G. Kanatzidis, I. Chung, B. Lee, and R.P. H. Chang, US-Patent 2013/0233377 A1 (2013).
[20] M.G. Kanatzidis, I. Chung, and K. Stoumpos, US-Patent 2013/0320836 A1 (2013).
[21] G. Kresse and D. Joubert, Phys. Rev. B **59**, 1758 (1999).
[22] P. E. Blöchl, Phys. Rev. B **50**, 17 953 (1994).
[23] J. P. Perdew, K. Burke, and M. Ernzerhof, Phys. Rev. Lett. **77**, 3865 (1996); *Erratum*: Phys. Rev. Lett. **78**, 1396 (1997).
[24] H. J. Monkhorst and James D. Pack, Phys. Rev. B **13**, 12 (1976).
[25] L. Huang and W. R. L. Lambrecht, Phys. Rev. B **88**, 165203 (2013).
[26] See supplementary material at http://dx.doi.org/10.1063/1.4927503 for the low lying configurations of CsSnI$_2$Cl, CsSnI$_2$Br, CsSnBr$_2$I, and CsSnBr$_2$Cl.